

Thermal Entanglement Between Atoms in the Four-Cavity Linear Chain Coupled by Single-Mode Fibers

Jun-Biao Wang¹ · Guo-Feng Zhang¹

Received: 20 February 2018 / Accepted: 8 May 2018 / Published online: 21 May 2018
© Springer Science+Business Media, LLC, part of Springer Nature 2018

Abstract Natural thermal entanglement between atoms of a linear arranged four coupled cavities system is studied. The results show that there is no thermal pairwise entanglement between atoms if atom-field interaction strength f or fiber-cavity coupling constant J equals to zero, both f and J can induce thermal pairwise entanglement in a certain range. Numerical simulations show that the nearest neighbor concurrence C_{AB} is always greater than alternate concurrence C_{AC} in the same condition. In addition, the effect of temperature T on the entanglement of alternate qubits is much stronger than the nearest neighbor qubits.

Keywords Quantum thermal entanglement · Concurrence · Coupled cavities system

1 Introduction

Entanglement is responsible for the non-local correlation, which is one of the most striking feature in quantum mechanics. It plays an essential role in the application of quantum communication and quantum computation [1–4], such as dense coding [2], quantum teleportation [3], quantum cryptographic protocols [4], etc. Consequently, studying the properties of entanglement is of particular importance for both fundamental research and practical applications.

A kind of interesting and innate entanglement, the so-called thermal entanglement (TE), has been widely studied in recent years. Comparing with other kinds of entanglements, TE is more stable than others due to it has taken thermal decoherence into account implicitly [5]. Besides that, TE demonstrates that entanglement can be generated thermally and persisted

✉ Guo-Feng Zhang
gf1978zhang@buaa.edu.cn

¹ Key Laboratory of Micro-Nano Measurement-Manipulation and Physics (Ministry of Education), School of Physics and Nuclear Energy Engineering, Beihang University, Xueyuan Road No. 37, Beijing 100191, China

in the thermodynamic limit [6, 7]. Since the seminal works by Arnesen [6] et al. and Nielsen [7], TE has been extensively investigated for different systems. The entanglement of non-equilibrium thermal states has been widely studied in [8–11]. Also the quantum teleportation scheme via thermal entangled states has been reported in [12–15]. Nevertheless, most of previous works are mainly limited to the Heisenberg spin chains. TE in the cavity quantum electrodynamics (cavity-QED) model is scarcely considered.

We know that the atom-photon interaction is one of essential approaches to realize entanglement for quantum information processing (QIP) and cavity-QED describes the coherent interaction between two-level atom and quantized cavity electromagnetic field. The cavity-QED model, which is different from other schemes (e.g., the spin chain model) by its advantages of easily addressing distinct cavities isolated from each other for avoiding cross-talk, and it has become a suitable candidate to encode quantum information since the atoms trapped inside cavities can have relatively long-lived atomic level [16–18]. Furthermore, the cavity-QED makes a good model to enable us control and measure the atom-field subsystem individually in the preparing process [19]. Hence, it has become a versatile and controllable platform for QIP (e.g., quantum logic gates [20] and teleportation [21] have been realized in cavity-QED platform).

The TE between nearest, next nearest in multiqubit Heisenberg spin chains was investigated in [22, 23]. These works have been revealed some novel properties, e.g., the pairwise entanglement undergoes two sudden changes, which may can be used as quantum entanglement switch [22]. These results inspire us to wonder whether the entanglement has some interesting properties in the framework of cavity-QED model. Recently, Huang et al. [24] have proposed an efficient scheme to generate multi-atom entangled states in coupled cavities system. The significant advantage of the scheme is the much less requirement of the interaction time, which can avoid decoherence as much as possible. Temperature can influence states of systems, including the atoms and the photons, and lead to change of entanglement [25]. From the practical point of view, with the technical support of laser cooling and trapping, we can separately control the trapped atoms in cavity and manipulate the atom-photon interaction with high accuracy. This motivated us to consider our current study. Based on cavity-QED model, the present paper is thus devoted to study the atomic subsystem entanglement of a linear arranged four coupled cavities system at an equilibrium temperature T .

The outline of the paper is as follows. Various measures of thermal entanglement, such as Wootters' concurrence C , i concurrence IC_i and global entanglement \mathcal{Q} are in detail introduced in the next section. Later, we present the physical model and the ground state pairwise entanglement in Section 3. The influences of system interaction parameters and environmental temperature on thermal entanglement are thoroughly discussed in Section 4. Finally, the summary is given in Section 5.

2 Measures of Thermal Entanglement

A quantum state, which is in thermal equilibrium at temperature T , can be represented by the density operator

$$\rho(T) = (1/Z) \exp(-H/kT), \quad (1)$$

with $Z = \text{Tr}[\exp(-H/kT)]$ is the partition function, H is the system Hamiltonian, k denotes the Boltzmann's constant and $k \equiv 1$ is assumed herein. Since $\rho(T)$ represents a thermal state, this entanglement is called thermal entanglement.

The convenient way to measure the entanglement of two qubits is by means of Wootters’ concurrence C [26]. Firstly, we can obtain the reduced density matrix $\rho_r(T)$ of two qubits by performing a partial trace over the remaining subsystems. Starting from the density matrix ρ_r , the Wootters’ concurrence is then calculated by

$$C = \max\{\lambda_1 - \lambda_2 - \lambda_3 - \lambda_4, 0\}, \tag{2}$$

where the quantities $\lambda_i (i = 1, 2, 3, 4)$ are the square roots of the eigenvalues of the operator

$$\varrho = \rho_r(\sigma_1^y \otimes \sigma_2^y)\rho_r^*(\sigma_1^y \otimes \sigma_2^y), \tag{3}$$

in descending order. ρ_r^* represents the complex conjugate of ρ_r . The concurrence is available, no matter whether ρ_r is pure or mixed [25]. The value of the concurrence C ranges from zero to one when the quantum state is changed from separable to maximally entangled state.

Besides the concurrence C , the global entanglement \mathcal{Q} also can be applied to quantify the entanglement of N -qubit quantum pure states. The global entanglement \mathcal{Q} was first introduced by Meyer and Wallach [27] and then reformulated by Brennen [28], which reads as

$$\mathcal{Q} = 2 \left[1 - (1/N) \sum_{i=1}^N \text{Tr}(\rho_i^2) \right], \tag{4}$$

with ρ_i , the density matrix, reduced to a single qubit i . The so-called i -concurrence IC_i [29, 30], which measures the entanglement between the single qubit i and the rest subsystem, is also directly related to the reduced density matrix ρ_i , and IC_i can be written as

$$IC_i = \sqrt{2[1 - \text{Tr}(\rho_i^2)]}, \tag{5}$$

based on (4) and (5) the global entanglement \mathcal{Q} can be rewritten as

$$\mathcal{Q} = (1/N) \sum_{i=1}^N IC_i^2, \tag{6}$$

here (6) elucidates the physical meaning of the global entanglement \mathcal{Q} as an average over the entanglement of each single qubit i against the rest subsystem.

3 The Model and the Ground State Pairwise Entanglement

3.1 The Model and Solutions

As illustrated in Fig. 1, we consider a physical system that four identical two-level atoms (labeled as A, B, C, D) are trapped respectively in four spatially separated adjacent equidistance single-mode cavities (labeled as I, II, III, IV), which are placed at a periodic linear chain and connected by three optical fibers. Each two-level atom (its atomic transition $|g\rangle \leftrightarrow |e\rangle$) experiences the same field environment and resonantly interacts with the field of its respective single-mode cavity via a one-photon hopping [18, 31–34]. Furthermore, in this scheme, we only consider the influence of equilibrium environment temperature on the system and ignore the other interactions between system and environment, i.e., cavity losses and fiber photon leakages have been ignored [18, 24].

Under the dipole and rotating-wave approximation (RWA) the atom-cavity interaction Hamiltonian is described by the Jaynes-Cumming model ($\hbar = 1$)

$$H_{a-c} = \sum_{i=1}^4 f_i (a_i^\dagger \sigma_{i-} + a_i \sigma_{i+}), \tag{7a}$$

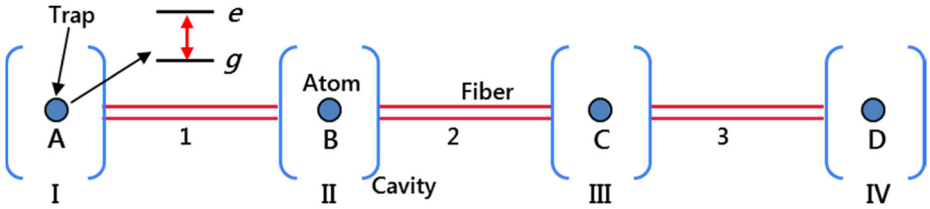


Fig. 1 (Color online) Schematic diagram of a linear arranged four coupled cavities system

where a_i^\dagger and a_i denote the creation and annihilation operator of field mode in the i th cavity, respectively. $\sigma_{i+} = |e\rangle_i \langle g|$ and $\sigma_{i-} = |g\rangle_i \langle e|$, respectively, represent the raising and lowering operator for the atomic system, with $|e\rangle_i(|g\rangle_i)$ being the excited (ground) states of the i th atom f_i is the interaction strength between i th atom and field mode of the i th cavity. Similarly, in the short-fiber limit, and only considering one resonant fiber mode interacts with the cavity mode [35], the coupling Hamiltonian between the fiber modes and the cavity fields can be approximated to ($\hbar = 1$)

$$H_{f-c} = \sum_{j=1}^3 J_j [b_j (a_j^\dagger + a_{j+1}^\dagger) + b_j^\dagger (a_j + a_{j+1})], \tag{7b}$$

where b_j^\dagger and b_j denote the creation and annihilation operator associated with the resonant mode of j th fiber, respectively. J_j is the coupling constant between fiber mode b_j and cavity mode a_j and a_{j+1} . Taking advantage of (7a) and (7b), one can acquire the total interaction Hamiltonian

$$H_I = H_{a-c} + H_{f-c} = \sum_{i=1}^4 f_i (a_i^\dagger \sigma_{i-} + a_i \sigma_{i+}) + \sum_{j=1}^3 J_j [b_j (a_j^\dagger + a_{j+1}^\dagger) + b_j^\dagger (a_j + a_{j+1})]. \tag{7}$$

Only considering one excitation number of the entire system case, the whole system evolves in subspace \forall , which can be spanned by the following basic state vectors:

$$\begin{aligned} |\varphi_1\rangle &= |eggg\rangle_a |0000\rangle_c |000\rangle_f, \\ |\varphi_2\rangle &= |gegg\rangle_a |0000\rangle_c |000\rangle_f, \\ |\varphi_3\rangle &= |ggeg\rangle_a |0000\rangle_c |000\rangle_f, \\ |\varphi_4\rangle &= |ggge\rangle_a |0000\rangle_c |000\rangle_f, \\ |\varphi_5\rangle &= |gggg\rangle_a |1000\rangle_c |000\rangle_f, \\ |\varphi_6\rangle &= |gggg\rangle_a |0100\rangle_c |000\rangle_f, \\ |\varphi_7\rangle &= |gggg\rangle_a |0010\rangle_c |000\rangle_f, \\ |\varphi_8\rangle &= |gggg\rangle_a |0001\rangle_c |000\rangle_f, \\ |\varphi_9\rangle &= |gggg\rangle_a |0000\rangle_c |100\rangle_f, \\ |\varphi_{10}\rangle &= |gggg\rangle_a |0000\rangle_c |010\rangle_f, \\ |\varphi_{11}\rangle &= |gggg\rangle_a |0000\rangle_c |001\rangle_f. \end{aligned} \tag{8}$$

where the subscript $\{a, c, f\}$ denotes the state of atoms, cavities mode and fibers mode, respectively. $|0\rangle$ and $|1\rangle$ represent the Fock state of resonant field mode.

For the sake of simplicity, we take $\forall f_i = f (i = 1, 2, 3, 4)$ and $\forall J_j = J (j = 1, 2, 3)$ (there should be no difficulty to achieve a homogeneous system experimentally [18]). In the following, we will work in units unless it is specially stressed. In the subspace \mathcal{V} , the eigenvalues of total Hamiltonian (7) are explicitly given by

$$\begin{aligned}
 E_1 &= E_2 = E_3 = 0, & E_4 &= -f, E_5 = f, \\
 E_6 &= -\sqrt{f^2 + 2J^2}, & E_7 &= \sqrt{f^2 + 2J^2}, \\
 E_8 &= -\sqrt{f^2 + (2 - \sqrt{2})J^2}, & E_9 &= \sqrt{f^2 + (2 - \sqrt{2})J^2}, \\
 E_{10} &= -\sqrt{f^2 + (2 + \sqrt{2})J^2}, & E_{11} &= \sqrt{f^2 + (2 + \sqrt{2})J^2}.
 \end{aligned} \tag{9}$$

Due to $E_1 = E_2 = E_3 = 0$, it is obvious that their eigenstates are three-fold degenerate. Taking advantage of Gram-Schmidt process, one can obtain the corresponding orthonormal eigenstates

$$\begin{aligned}
 |\phi_1\rangle &= J/\sqrt{f^2 + 2J^2}(|\varphi_3\rangle + |\varphi_4\rangle - f/\sqrt{f^2 + 2J^2}|\varphi_{11}\rangle), \\
 |\phi_2\rangle &= A_{2,2}|\varphi_2\rangle + A_{2,3}|\varphi_3\rangle + A_{2,4}|\varphi_4\rangle + A_{2,10}|\varphi_{10}\rangle + A_{2,11}|\varphi_{11}\rangle, \\
 |\phi_3\rangle &= A_{3,1}|\varphi_1\rangle + A_{3,2}|\varphi_2\rangle + A_{3,3}|\varphi_3\rangle + A_{3,4}|\varphi_4\rangle + A_{3,9}|\varphi_9\rangle + A_{3,10}|\varphi_{10}\rangle + A_{3,11}|\varphi_{11}\rangle, \\
 |\phi_4\rangle &= 1/2\sqrt{2}(|\varphi_1\rangle - |\varphi_2\rangle + |\varphi_3\rangle - |\varphi_4\rangle - |\varphi_5\rangle + |\varphi_6\rangle - |\varphi_7\rangle + |\varphi_8\rangle), \\
 |\phi_5\rangle &= 1/2\sqrt{2}(-|\varphi_1\rangle + |\varphi_2\rangle - |\varphi_3\rangle + |\varphi_4\rangle - |\varphi_5\rangle + |\varphi_6\rangle - |\varphi_7\rangle + |\varphi_8\rangle), \\
 |\phi_6\rangle &= f/2\sqrt{2f^2 + 4J^2}(-|\varphi_1\rangle - |\varphi_2\rangle + |\varphi_3\rangle + |\varphi_4\rangle) + 1/2\sqrt{2}(|\varphi_5\rangle + |\varphi_6\rangle - |\varphi_7\rangle - |\varphi_8\rangle) \\
 &\quad + J/\sqrt{2f^2 + 4J^2}(-|\varphi_9\rangle + |\varphi_{11}\rangle), \\
 |\phi_7\rangle &= f/2\sqrt{2f^2 + 4J^2}(-|\varphi_1\rangle - |\varphi_2\rangle + |\varphi_3\rangle + |\varphi_4\rangle) - 1/2\sqrt{2}(|\varphi_5\rangle + |\varphi_6\rangle - |\varphi_7\rangle - |\varphi_8\rangle) \\
 &\quad + J/\sqrt{2f^2 + 4J^2}(-|\varphi_9\rangle + |\varphi_{11}\rangle), \\
 |\phi_8\rangle &= A_{8,1}(|\varphi_1\rangle + |\varphi_4\rangle + A_{8,2}|\varphi_2\rangle + |\varphi_3\rangle) - \sqrt{2 + \sqrt{2}}/4(|\varphi_5\rangle + |\varphi_8\rangle) \\
 &\quad + \sqrt{2 - \sqrt{2}}/4(|\varphi_6\rangle + |\varphi_7\rangle) + A_{8,9}(|\varphi_9\rangle + |\varphi_{11}\rangle) + A_{8,10}|\varphi_{10}\rangle, \\
 |\phi_9\rangle &= A_{9,1}(|\varphi_1\rangle + |\varphi_4\rangle - A_{9,2}|\varphi_2\rangle + |\varphi_3\rangle) + \sqrt{2 + \sqrt{2}}/4(|\varphi_5\rangle + |\varphi_8\rangle) \\
 &\quad - \sqrt{2 - \sqrt{2}}/4(|\varphi_6\rangle + |\varphi_7\rangle) + A_{9,9}(|\varphi_9\rangle + |\varphi_{11}\rangle) - A_{9,10}|\varphi_{10}\rangle, \\
 |\phi_{10}\rangle &= A_{10,1}(|\varphi_1\rangle + |\varphi_4\rangle + A_{10,2}|\varphi_2\rangle + |\varphi_3\rangle) - \sqrt{2 - \sqrt{2}}/4(|\varphi_5\rangle + |\varphi_8\rangle) \\
 &\quad - \sqrt{2 + \sqrt{2}}/4(|\varphi_6\rangle + |\varphi_7\rangle) + A_{10,9}(|\varphi_9\rangle + |\varphi_{11}\rangle) + A_{10,10}|\varphi_{10}\rangle, \\
 |\phi_{11}\rangle &= A_{11,1}(|\varphi_1\rangle + |\varphi_4\rangle + A_{11,2}|\varphi_2\rangle + |\varphi_3\rangle) + \sqrt{2 - \sqrt{2}}/4(|\varphi_5\rangle + |\varphi_8\rangle) \\
 &\quad + \sqrt{2 + \sqrt{2}}/4(|\varphi_6\rangle + |\varphi_7\rangle) + A_{11,9}(|\varphi_9\rangle + |\varphi_{11}\rangle) + A_{11,10}|\varphi_{10}\rangle,
 \end{aligned} \tag{10}$$

in which $A_{m,n}$ stands for the normalized factor of the eigenstates. The integer subscript $\{m, n\}$ both range from to 11. For the reason of succinct presentation, we omit the analytical form of $A_{m,n}$.

3.2 The Ground State Pairwise Entanglement

The system is in the ground state when $T = 0$. From (9), we can find that the ground-state energy is $E_{10} = -\sqrt{f^2 + (2 + \sqrt{2})J^2}$. Considering two different types pairwise entanglement, we denote the entanglement of the nearest neighbor qubits (i.e., atom A , B) and of the alternate qubits (i.e., atom A , C) by C_{AB} and C_{AC} , respectively. With the help of (2), (3) and ground state $|\phi_{10}\rangle$, it is straightforward to obtain C_{AB} and C_{AC}

$$C_{AB} = C_{AC} = 2A_{10,1} * A_{10,2} = \frac{(2 + \sqrt{2})f^2}{8(1 + \sqrt{2})f^2 + 8(4 + 3\sqrt{2})J^2}, \tag{11}$$

with the two normalized factors of $|\phi_{10}\rangle$, i.e., $A_{10,1} = \frac{f}{2\sqrt{2(2+\sqrt{2})f^2+4(3+2\sqrt{2})J^2}}$ and $A_{10,2} = \frac{(2+\sqrt{2})f}{4\sqrt{(2+\sqrt{2})f^2+2(3+2\sqrt{2})J^2}}$. The (11) means that the nearest neighbor concurrence equals to the alternate concurrence, namely, the value of concurrence is independent of the sites of atoms for the ground state case.

The ground-state concurrence C_{AB} and C_{AC} as functions of fiber-cavity coupling constant J and atom-cavity interaction strength f are depicted in Fig. 2a. From Fig. 2a, one can see that C_{AB} and C_{AC} are monotone increasing as a function of the atom-cavity interaction strength f . Contrarily, as the fiber-cavity coupling constant J increases, the concurrence

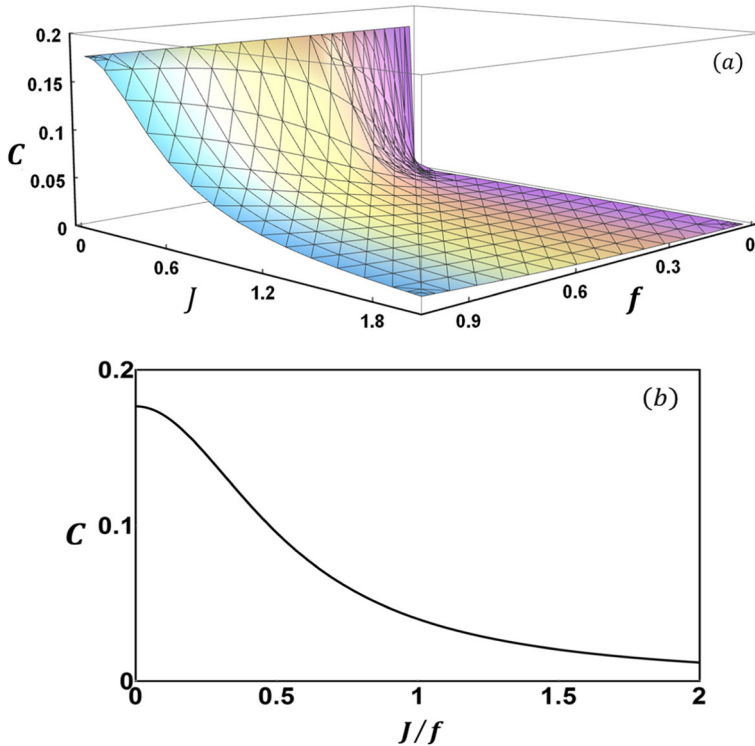


Fig. 2 (Color online) The ground-state concurrence C_{AB} and C_{AC} are plotted vs. J and f in (a); C_{AB} and C_{AC} are plotted vs. the ratio J/f in (b)

decreases. Besides that, when J or f equals to zero, there is no pairwise entanglement between atoms in ground state. In Fig. 2b, we give the plot of ground-state concurrence as a function of the ratio J/f . Evidently, the entanglement is decreasing with increasing ratio to be zero; the maximum entanglement value is about 0.177 when the ratio is extremely close to zero. Therefore, it means that if we keep $f \gg J$, then we will induce high quality pairwise entanglement of ground state in certain experimental situations. The further information about how the ratio J/f effects on the behaviors of thermal pairwise entanglement between atoms when $T \neq 0$ will be discussed later.

4 The Thermal Entanglement

In the following, we mainly focus on the effect of the fiber-cavity coupling constant J , atom-field interaction strength f and temperature T on the pairwise thermal entanglement from different perspectives. In addition, we investigate the global entanglement \mathcal{Q} and the i -concurrence IC_i as a function of J and f for a low temperature case $T = 0.01$.

4.1 The Pairwise Thermal Entanglement

If we consider the thermal entanglement between the nearest neighbor qubits (i.e., atom A, B), we need to obtain the reduced density matrix ρ_{AB} by tracing out all the remaining degrees of freedom for the other subsystems [33]. Hence we have $\rho_{AB} = \text{Tr}_{R-S}\rho(T)$ (the subscript $R - S$ stands for the remaining subsystems), in the standard atomic basis $\{|gg\rangle, |ge\rangle, |eg\rangle, |ee\rangle\}$, one can acquire

$$\rho_{AB}(T) = \frac{1}{Z} \begin{pmatrix} \rho_{11} & 0 & 0 & 0 \\ 0 & \rho_{22} & \rho_{23} & 0 \\ 0 & \rho_{23}^* & \rho_{33} & 0 \\ 0 & 0 & 0 & 0 \end{pmatrix}, \tag{12}$$

where $\rho_{ij}(i, j = 1, 2, 3, 4)$ represents the matrix element. Taking advantage of (12) and the definition of concurrence, one can acquire the nearest neighbor concurrence C_{AB} at the finite temperature,

$$C_{AB} = 2\sqrt{|\rho_{23}|^2/Z}, \tag{13}$$

in which the partition function $Z = 3 + 2 \cosh(f/T) + 2 \cosh(\mu/T) + 2 \cosh(\eta/T) + \cosh(\xi/T)$. We also obtain the matrix element ρ_{23}, ρ_{23}^* in the basis $\{|gg\rangle, |ge\rangle, |eg\rangle, |ee\rangle\}$

$$\begin{aligned} \rho_{23} = \rho_{23}^* = & \frac{1}{8} \left(-2 \cosh\left(\frac{f}{T}\right) + \frac{2f^2 \cosh\left(\frac{\mu}{T}\right)}{\mu^2} + \frac{\sqrt{2}f^2 \cosh\left(\frac{\xi}{T}\right)}{\xi^2} - \frac{\sqrt{2}f^2 \cosh\left(\frac{\eta}{T}\right)}{\eta^2} \right) \\ & + \frac{J^2(f^4 + 3f^2J^2 + J^4)}{\mu^2\xi^2\eta^2} \end{aligned} \tag{14}$$

with the elements

$$\begin{aligned} \mu &= \sqrt{f^2 + 2J^2}, \\ \xi &= \sqrt{f^2 + (\sqrt{2} + 2)J^2}, \\ \eta &= \sqrt{f^2 - (\sqrt{2} - 2)J^2}. \end{aligned} \tag{15}$$

Similarly, for the alternate qubits (i.e., atom A, C), we also can calculate $\rho_{AC}(T)$ and obtain the alternate concurrence C_{AC}

$$\rho_{AC}(T) = \frac{1}{Z} \begin{pmatrix} \lambda_{11} & 0 & 0 & 0 \\ 0 & \lambda_{22} & \lambda_{23} & 0 \\ 0 & \lambda_{23}^* & \lambda_{33} & 0 \\ 0 & 0 & 0 & 0 \end{pmatrix}, \tag{16}$$

$$C_{AC} = 2\sqrt{|\lambda_{23}|^2/Z}, \tag{17}$$

with the matrix element $\lambda_{23}, \lambda_{23}^*$

$$\lambda_{23} = \lambda_{23}^* = \frac{1}{8} \left(2 \cosh\left(\frac{f}{T}\right) - \frac{2f^2 \cosh\left(\frac{\mu}{T}\right)}{\mu^2} + \frac{\sqrt{2}f^2 \cosh\left(\frac{\xi}{T}\right)}{\xi^2} - \frac{\sqrt{2}f^2 \cosh\left(\frac{\eta}{T}\right)}{\eta^2} \right) - \frac{J^4(f^2 + J^2)}{\mu^2 \xi^2 \eta^2} \tag{18}$$

Based on numerical results of C_{AB} and C_{AC} , the evolution of C_{AB} (solid line) and C_{AC} (dashed line) with respect to temperature T are illustrated in Fig. 3a with $f = 1.5$ for various values of J and in Fig. 3b with $J = 1.5$ for different values of f , respectively. As depicted in Fig. 3, C_{AB} shares the same initial entanglement value with C_{AC} at $T = 0$, where the system is still in its ground state $|\phi_{10}\rangle$. As the thermal fluctuation is introduced into the system, the ground state will be mixed with some excited states. This effect will change the magnitude of entanglement. As the temperature T increases, the entanglement between the alternate qubits C_{AC} drops off monotonically until disappears. Contrarily, the nearest neighbor concurrence C_{AB} in the beginning increases with T to its maximum value C_{AB}^{\max} , then decays off gradually due to the thermal decoherence.

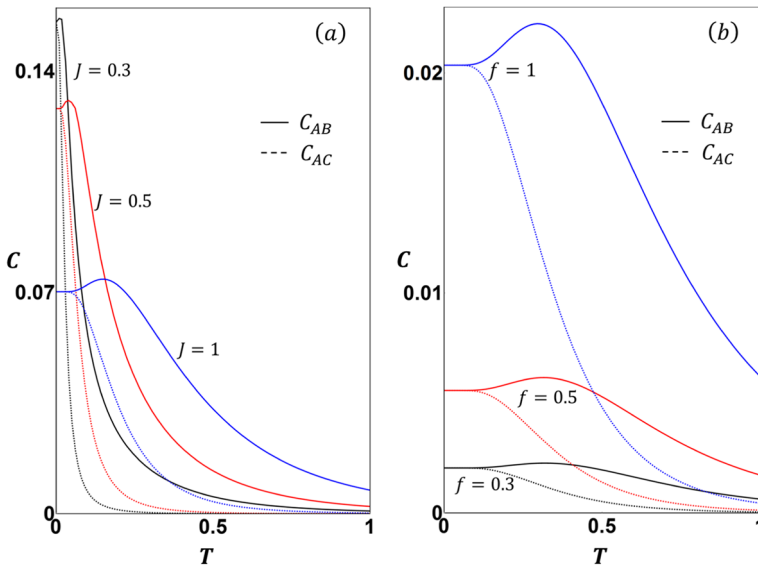


Fig. 3 (Color online) C_{AB} (solid line) and C_{AC} (dashed line) are plotted vs. temperature T , for $f = 1.5$ with $J = 0.3, 0.5, 1.0$ (Curve color: black, red, blue, respectively) in (a) and for $J = 1.5$ with $f = 0.3, 0.5, 1.0$ (Curve color: black, red, blue, respectively) in (b)

As is evident from Fig. 3, the curve of C_{AC} varies greater than C_{AB} as a function of temperature T , it explicitly reflects that the effect of temperature T on thermal pairwise entanglement between atoms is much stronger for alternate qubits than nearest neighbor qubits, although the interaction between the nearest neighbor qubits is much stronger. This result is consistent with the previous study for Heisenberg XX chain case [22].

Furthermore, for $f = 1.5$ in Fig. 3a, it can be seen that C_{AB} and C_{AC} will be decreased with the increase in fiber-cavity coupling J at a fixed temperature. The maximum value C_{AB}^{\max} as well as the temperature T_0 at which it occurs, are also shown to strongly depend upon J . Besides, in Fig. 3b, for the case of $J = 1.5$, C_{AB} and C_{AC} increase with the stronger atom-field interaction, and the C_{AB}^{\max} and its corresponding T_0 are also strongly depend upon f .

By comparing Fig. 3a and b, we can see that as the value of J/f becomes smaller, both C_{AB} and C_{AC} become greater. On the contrary, the existence region of entanglement is diminishing since the decay rate increases as J/f decreases. Therefore, it is reasonable to conjecture that the ratio J/f not only affects the ground-state pairwise entanglement, but also influences the quality of thermal pairwise entanglement. That is to say, we may maintain a robust atomic subsystem entanglement by adjusting suitable system parameters.

In what follows, we give the results about how the C_{AB} and C_{AC} vary with J (in Fig. 4a) and f (in Fig. 4b) for different temperatures (i.e., $T = 0.01, 0.1, 0.5$). From Fig. 4, it is easily found that there is no thermal pairwise entanglement between atoms if f or J equals to zero, which can be explained that since the correlation between atoms is vanish, each of atoms is not entangled with another atom. In addition, as shown in Fig. 4, as the strength of interaction f and J increases, both C_{AB} and C_{AC} initially increase rapidly to reach their maximum value C_{\max} and then gradually decrease to zero. Accordingly, the maximum value C_{\max} decreases with the increasing temperature.

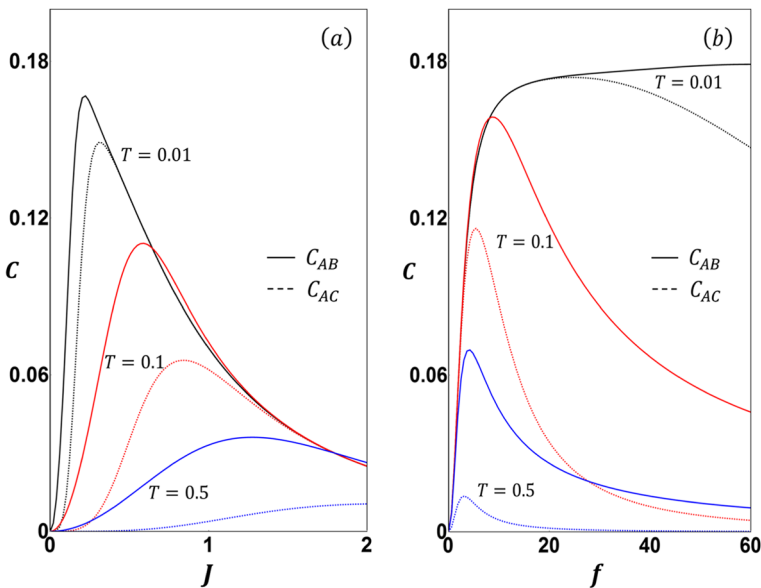


Fig. 4 (Color online) C_{AB} (solid line) and C_{AC} (dashed line) are plotted vs. J , for $f = 1.5$ in (a); C_{AB} and C_{AC} are plotted vs. f for $J = 1.5$ in (b). Both in (a) and (b), the curves are plotted with various temperature T (from top to bottom $T = 0.01, 0.1, 0.5$)

We also observe from Fig. 4 that when the value of J (in Fig. 4a) or f (in Fig. 4b) changes, the thermal entanglement of nearest-neighbor qubits always varies greater than that of alternate qubits. That is to say, since the interaction between the nearest-neighbor qubits is more directly and stronger the effects of J and f on C_{AB} is much stronger than C_{AC} . Meanwhile, as is evident from Figs. 3a–b and 4a–b, the value of C_{AB} is always greater than that of C_{AC} in the same condition. It implies that the further the qubits sites are, lesser is the magnitude of the entanglement between them.

4.2 Behaviors of the Global Entanglement \mathcal{Q} and i -Concurrence IC_i When $T = 0.01$

In this section, we investigate in detail the behaviors of the global entanglement \mathcal{Q} between atoms and i -concurrence IC_i of each atom for a low temperature ($T = 0.01$) case (so that the entanglement is predominantly determined by the ground state). Due to the sites of qubits are of symmetry, each IC_i satisfies the following relations:

$$\begin{aligned} IC_1 &= IC_4, \\ IC_2 &= IC_3. \end{aligned} \tag{19}$$

By virtue of the definition of i -concurrence [see (5)], we can obtain the reduced density matrix ρ_i of a subsystem i (i.e., i th atom) in the basis $\{|g\rangle, |e\rangle\}$

$$\rho_i = \begin{pmatrix} 1 - \rho_{ii} & 0 \\ 0 & \rho_{ii} \end{pmatrix}, \tag{20}$$

where ρ_{ii} is the diagonal matrix element of given ρ in (1). ρ stands for the thermal equilibrium state of total system. It is straightforward to calculate: $\text{Tr}(\rho_i^2) = 2\rho_{ii}^2 - 2\rho_{ii} + 1$. Thus, we find

$$IC_i = 2\sqrt{\rho_{ii} - \rho_{ii}^2}. \tag{21}$$

In addition, based on the definition of global entanglement \mathcal{Q} , putting (21) into (6) and taking $N = 4$, one can obtain

$$\mathcal{Q} = \sum_{i=1}^4 \rho_{ii} - \rho_{ii}^2. \tag{22}$$

Based on the above analysis, taking $f = 1.5$ and $T = 0.01$, we can obtain the evolution of global entanglement \mathcal{Q} and i -concurrence IC_i with respect to J , as depicted Fig. 5a. From the figure, it is found that \mathcal{Q} and $IC_1(IC_4)$ decrease monotonically with the increasing value of J . Contrarily, $IC_2(IC_3)$ at first increases to its maximum value, which equals to 0.79, and then decreases to zero. Note that, when $J = 0$ is given, there is no interaction between fiber and cavity (i.e., no information exchange among the them). According to the physical meaning of \mathcal{Q} and IC_i , we have $\mathcal{Q} = IC_i = 0$, thus, there are discontinuity points at $J = 0$ in Fig. 5a. Meanwhile, in Fig. 5b, we show the dependence of \mathcal{Q} and IC_i on f when $T = 0.01$ and $J = 1.5$. If we assume that atom-field interaction vanishes (i.e., $f = 0$) in Fig. 5b, there is also no i -concurrence and the global entanglement between atoms. Therefore, by combining with the previous results in Fig. 4a and b, we can conclude that there should be no entanglement for the atomic subsystem in the case of $f = 0$ or $J = 0$.

We also observe in Fig. 5b that the global entanglement \mathcal{Q} and each i -concurrence IC_i will initially increase to their maximum value E_{\max} as the atom-field interaction goes up.

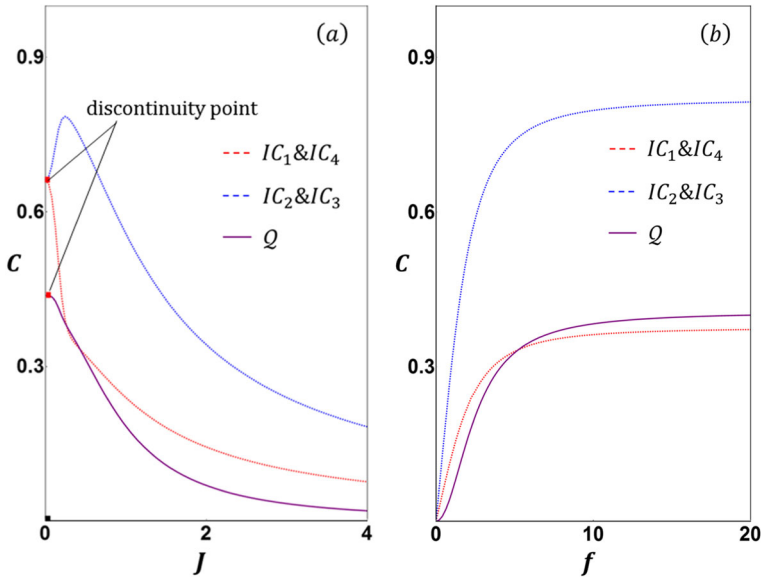


Fig. 5 (Color online) With a low temperature $T = 0.01$. Q (purple solid line), $IC_1 \& IC_4$ (purple solid line) and $IC_2 \& IC_3$ (purple solid line) are plotted vs. J , for $f = 1.5$ in (a); Q and each IC_i are plotted vs. f , for $J = 1.5$ in (b). There are discontinuity points at $J = 0$ in (a)

In order to forecast the changeable trend of Q and each IC_i , the first step is to obtain their maximum value E_{\max} and the corresponding parameter f_0^{\max} . After a straight calculation, we obtain

$$\begin{aligned}
 f_0^{\max} &\rightarrow 33660.6 & E_{\max} &\approx 0.6609, & \text{for } IC_1, IC_4; \\
 f_0^{\max} &\rightarrow 32.1 & E_{\max} &\approx 0.8163, & \text{for } IC_2, IC_3; \\
 f_0^{\max} &\rightarrow 284976 & E_{\max} &= 0.4375, & \text{for } Q;
 \end{aligned} \tag{23}$$

Besides that, in the limit of $f \rightarrow \infty$, one can acquire Q and each IC_i : $\lim_{f \rightarrow \infty} IC_i \approx 0.6614$, $\lim_{f \rightarrow \infty} Q \approx 0.4375$. Hence $IC_2(IC_3)$ will decrease after the increasing parameter f exceed f_0^{\max} . From the two figures, we also find that atomic global entanglement and i -concurrence will keep a high value when the atom-field interaction is far stronger than fiber-cavity coupling.

5 Conclusions

To summarize, in a linear arranged four coupled cavities system, we have investigated the thermal entanglement between atoms and thoroughly discussed the dependence of the thermal entanglement on the atom-field interaction strength f , fiber-cavity coupling constant J and temperature as well. We have found that the atomic entanglement exists at zero temperature and the concurrence are the same for both nearest neighbor qubits and alternate qubits.

Our results indicate that the temperature affects the alternate qubits concurrence C_{AC} is much stronger than nearest neighbor qubits C_{AB} , which accords with the conclusions in [22]. In addition, we also showed that in the same condition the further the qubits sites are, lesser is the magnitude of the entanglement between them. Based on numerical evidences, we have conjectured that both the ground state entanglement and thermal entanglement strongly depends on J and f , especially their ratio J/f . Moreover, the robust entanglement can be prepared experimentally by choosing an appropriate interaction parameter and lowering temperature. We also have studied the atomic global entanglement Q and i -concurrence IC_i for a low temperature.

For a realistic quantum system, the influence of dissipation cannot be completely ignored [36], how we preserve entanglement is still a big challenge for current technology. In the future we will investigate how to create stable thermal entanglement in the case of decoherence effect. We expect that our investigation of the results in the framework of coupled cavities systems broaden the theoretical study of thermal entanglement and related applications.

Acknowledgements This work is supported by the National Natural Science Foundation of China (Grant No. 11574022).

References

1. Bennett, C.H., DiVincenzo, D.P.: Nature **404**, 247 (2000)
2. Braunstein, S.L., Kimble, H.J.: Phys. Rev. A **61**, 042302 (2000)
3. Bennett, C.H., Brassard, G., Crépeau, C., Jozsa, R., Peres, A., Wootters, W.K.: Phys. Rev. Lett. **70**, 1895 (1993)
4. Ekert, A.K.: Phys. Rev. Lett. **67**, 661 (1991)
5. Zhang, G.-F., Li, S.-S.: Phys. Rev. A **72**, 034302 (2005)
6. Arnesen, M.C., Bose, S., Vedral, V.: Phys. Rev. Lett. **87**, 017901 (2001)
7. Nielsen, M.A., Chuang, I.L.: Quantum Computation and Quantum Information. Cambridge University Press, Cambridge (2000)
8. Quiroga, L., Rodríguez, F.J., Ramírez, M.E., París, R.: Phys. Rev. A **75**, 032308 (2007)
9. Huang, X.L., Guo, J.L., Yi, X.X.: Phys. Rev. A **80**, 054301 (2009)
10. Pumulo, N., Sinayskiy, I., Petruccione, F.: Phys. Lett. A **375**, 3157 (2011)
11. Bellomo, B., Antezza, M.: Phys. Rev. A **91**, 042124 (2015)
12. Yeo, Y.: Phys. Rev. A **66**, 062312 (2002)
13. Zhang, G.-F.: Phys. Rev. A **75**, 034304 (2007)
14. Qin, W., Guo, J.-L.: Theor. Phys. **54**, 2386 (2015)
15. Fortes, R., Rigolin, G.: Rev. A **96**, 022315 (2017)
16. Angelakis, D.G., Santos, M.F., Bose, S.: Phys. Rev. A **76**, 031805(R) (2007)
17. Ogden, C.D., Irish, E.K., Kim, M.S.: Phys. Rev. A **78**, 063805 (2008)
18. Yabu-Uti, B.F.C., Roversi, J.A.: Quantum Inf. Process. **12**, 189 (2013)
19. Abdel-Aty, M.: Prog. Quant. Electron. **31**, 1 (2007)
20. Pellizzari, T., Gardiner, S.A., Cirac, J.I., Zoller, P.: Model. Phys. Rev. Lett. **75**, 3788 (1995)
21. Zheng, S.-B., Guo, G.-C.: Phys. Rev. Lett. **85**, 2392 (2000)
22. Cao, M., Zhu, S.Q.: Phys. Rev. A **71**, 034311 (2005)
23. Wu, K.-D., Zhou, B., Cao, W.-Q.: Phys. Lett. A **362**, 381 (2007)
24. Huang, X.-B., Zhong, Z.-R., Chen, Y.-H.: Quantum Inf. Process. **14**, 4475 (2015)
25. Abbasi, M.R.: Phys. A **426**, 1 (2015)
26. Wootters, W.K.: Phys. Rev. Lett. **80**, 2245 (1998)
27. Meyer, D.A., Wallach, N.R.: J. Math. Phys. **43**, 4273 (2002)
28. Brennen, G.K.: Quantum Inf. Comput. **3**, 619 (2003)
29. Rungta, P., Bužek, V., Caves, C.M., Hillery, M., Milburn, G.J.: Phys. Rev. A **64**, 042315 (2001)
30. Endrejat, J., Büttner, H.: Phys. Rev. A **71**, 012305 (2005)

31. Cetina, M., Bylinskii, A., Karpa, L., Gangloff, D., Beck, K.M., Ge, Y., Scholz, M., Grier, A.T., Chuang, I., Vuletić, V.: *New J. Phys.* **15**, 053001 (2013)
32. Ahmed, A.H.M., Cheong, L.Y., Zakaria, N., Metwally, N., Eleuch, H.: *AIP Conf. Proc.* **1482**, 373 (2012)
33. Abdel-Aty, A.H., Zakaria, N., Cheong, L.Y., Metwally, N.: *J. Comput. Theor. Nanosci.* **12**, 2213 (2015)
34. Siegle, T., Schierle, S., Kraemmer, S., Richter, B., Wondimu, S.F., Schuch, P., Koos, C., Kalt, H.: *Light Sci. Appl.* **6**, e16224 (2017)
35. Ye, J., Vernooy, D.W., Kimble, H.J.: *Phys. Rev. Lett.* **83**, 4987 (1999)
36. Homid, A.H., Abdel-Aty, A., Abdel-Aty, M., Badawi, A., Obada, A.-S.F.: *Opt. Soc. Am. B* **32**, 2025 (2015)